ASM Sc. J., 11, Special Issue 2, 2018 for SANREM, 49-65

Earthquake and Tsunami Propagation Scenario in Tawau, Sabah - Evaluation of The North Sulawesi Fault Parameter

Ahmad Khairut Termizi[1,2,3], Felix Tongkul[2,3], Rodeano Roslee[2,3*]

[1]*Minerals and Geoscience Department of Malaysia (JMG-Malaysia), Jalan Penampang, 88999 Kota Kinabalu, Sabah, Malaysia*

[2]*Natural Disaster Research Centre (NDRC), University Malaysia Sabah (UMS), Jalan UMS, 88400 Kota Kinabalu, Sabah, Malaysia.*

[3]*Faculty of Science and Natural Resources (FSSA), University Malaysia Sabah (UMS), Jalan UMS, 88400 Kota Kinabalu, Sabah, Malaysia*

This study integrates analytical earthquake parameters with tsunami simulation application (TUNAMI-N2) and GIS (Geographic Information System). A total of 350 modelling on six earthquake parameters was carried out and a total of 79 observation segments was used to categorize waves height and to classify the level of tsunami threat in Tawau. Slip magnitude is the most sensitive parameter which contributes to the increase in wave height of 0.06m in the case of Northern Sulawesi. Every 1km change in fault width will contribute to a change of 0.05 waves height in the case of Northern Sulawesi. Changes in the value of rake and dip angles, fault length, and focal depth do not show consistent and significant changes in wave heights.

Keywords: Celebes Sea Tsunami, TUNAMI-N2, North Sulawesi Fault

I. INTRODUCTION

The tsunami incidents resulting from the earthquake generated by active faults have various situations, which is measured based on the four major tsunami parameters ie tsunami height, inundation, high rate of the tsunami, and tsunami creep periods to the point of observation (Behren, 2007). The scenario that applies to each change of tsunami parameter is directly related to the cause of the tsunami.

To find out the behavior of the tsunami wave creep and creep on the coast of Bandar Tawau, the study has provided a realistic domain model with a hypothetical earthquake parameter. This simulation is done by considering six of the seven earthquake parameters such as slip magnitude, fault length, fault width, angle, rake angle, and depth). The parameters for the direction of the jut is not taken into account in the determination of this tsunamigenic earthquake. This is to give a true picture of the fault. The fault state in the analysis of sensitivity determination is approaching the realistic case with six parameters involved change systematically, while the direction of the jitter is constant. If changes are made to the direction of the fault step, this condition will indirectly alter the realistic nature of the fault.

Determination of the sensitivity level of fault parameters is measured by recording the height of the tsunami and creep periods at five predetermined observation points. In this simulation, the inundation and elevation of the

*Corresponding author's e-mail: rodeano@ums.edu.my

inundation are not taken as a determination as the function of the TUNAMI-N2 model is limited only to propagation in the ocean alone, the advanced model is required to adopt the entire tsunami parameter as the assessment measure scale. Only relevant readings are recorded to ensure that the analysis is accurate and guarantees the validity of the study data.

II. TSUNAMI INDUCED EARTHQUAKE

Among the sources of tsunami generation, the earthquake is a major cause and contributes most to the tsunami generation (Latief, 2000). This study will detail the tsunami created by the earthquake. This takes into account the location of the study area, Tawau district. Located opposite the open sea of Celebes and surrounded by active faults and seagrasses potentially experiencing an earthquake and subsequently generating a tsunami (Raj, 2007). The earthquake that caused the tsunami was a seismic earthquake epicenter located in the ocean and has a depth of ephemeral (hypocentre) epicenter (approaching or standing on the surface of the ocean's crust). Figure 1 shows the difference between the depth of the earthquake point (hypocentre) and epicenter point location.

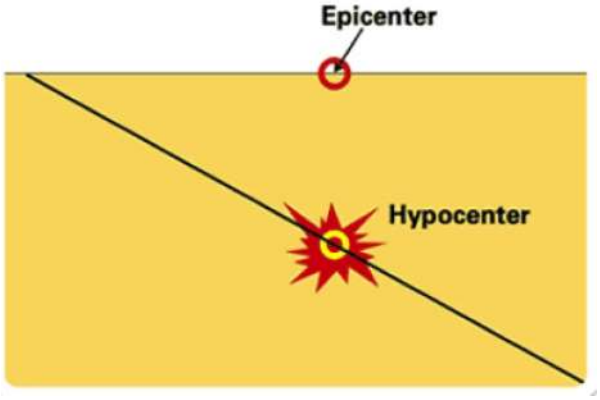

Figure 1: Location of epicenter and hypocenter of the earthquake (International Tsunami Information center ITIC, 2007)

The earthquake does not exist with just one point of the earthquake, it is followed by several other earthquake events where the magnitude of the magnitude is smaller. A tectonic earthquake that has the potential to generate tsunami waves is also known as a tsunamigenic earthquake. Not all earthquakes happen to be able to generate tsunami waves. Identified some of the characteristics of the earthquake-tsunami (tsunami):

a. Epicenter location is in the sea. This is because the earthquake that occurs on the ground cannot afford to balance the balance on the surface of the sea and no energy exists to be transferred to the body of water.
b. The depth of the earthquake center (hypocenter) is relatively shallow, this occurs at a depth of less than 100km from the surface of the sea floor. An earthquake occurring at a depth of less than 70 km along the subduction zone is capable of generating a large tsunami.

c. Has a magnitude of 7.5 on the scale of Richter and above, capable of producing a tsunami destroyer (ITIC, 2007).
d. Actual fault mechanisms resulting in seawater deflation or dislocation.

There are three types of faults that allow the formation of earthquakes ie convergent faults, normal faults, and divergent (Figure 2). Tectonic earthquakes are earthquakes that are related to the deformation of the crust. In the event of an underwater earthquake, the waters above the deformation zone swirl away from the stability position. Changes in the oceanic crust in the subduction zone will result in a tsunami.

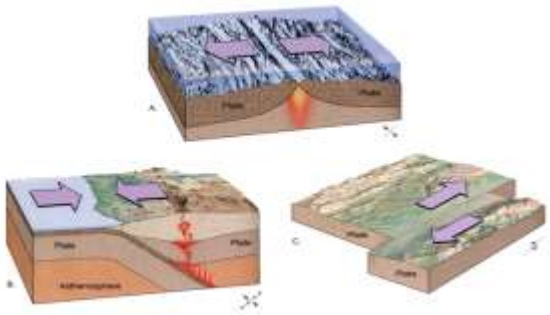

Figure 2: Type of faults that can generate earthquake (A. Convergent, B. Divergent, C. Normal Fault) (Yalciner, 2006)

In order to produce deformation on the seafloor, the earthquake should have a large, momentous moment with a shallow depth of hypocenter. The momentous moment will calculate the amount of energy released by the earthquake taking into account the displacement that occurs in the movement along the fault and the surface area of the fault which is undergoing movement. Moment magnitude is not suitable for a small-scale earthquake because relative displacement is small and insignificant. The relationship between the moment of momentum and deformation is formulated as below:

$$Mo = \mu.A.D \quad (1)$$

Mo = seismic moment (Nm)
M = rigidity (the value of the power of the object, the harder the energy then the energy needed to move it bigger, then the moment of the moment is bigger) (N/m²)
A = Fault width (m²)
D = deformation (m)

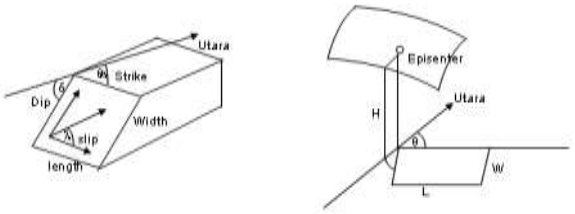

Figure 2: H = Depth, L = Length, W = Width, θ = Strike, δ = Dip, λ = Slip (Snoke, 1989)

Seismic parameters that need to be known in relation to tsunami formation are:

a. The moment of seismic.
b. Location and seismic depth (epicenter & hypocenter).
c. Mechanics and fault geometry (Figure 3).

III. TSUNAMI WAVE PARAMETERS

The tsunami is one of a series of ocean waves with very large wavelengths over a long period of

time. The tsunami is caused by the transfer of waves through the body of the water as a result of the sudden disruption. The tsunami can generally be classified into two main types, the local Tsunami, and the region's tsunami, also known as the long-distance tsunami.

Local tsunami is a tsunami that occurs in a position not far from the position where the earthquake occurred. Impacts of devastation through the tsunami are limited only to the coast within a radius of 100km from the source. This local tsunami is usually caused by an earthquake that may occur due to landslides or volcanic lava flows from the volcano that disturbs the body of water.

The region's tsunami is generally able to impact the destruction of certain geographical areas within a radius of 1,000km from the source. The tsunami region sometimes has a very limited impact and is a local tsunami in its outer territory. Local and regional tsunamis have devastated many casualties and property destruction. Recorded between 1975 and 2005 there were 22 incidents of local tsunamis and regions in the Pacific and surrounding seas that destroyed and killed. Apart from local tsunamis and tsunami regions, there is also a tsunami destroyer known as Teletsunami or Long Distance Tsunami. This type of tsunami is rare but the impact of the tsunami is very strong and has an impact beyond the regional tsunami radius of more than 1000km. This remote teletsunami or tsunami formation began as a local tsunami which had a major impact on the area around the earthquake source. As the force that drives the tsunami is on a large scale then this tsunami wave spread across the ocean niche. With the energetic power of teletsunami, it is able to impact the beaches that are located more than 1000km from the source of the earthquake. According to ITCI recorded in the last 200 years, there were at least 21 major teletsunami occurrences.

The tsunami waves generated by the earthquake will spread through deep-sea waters and further into the shallow area when approaching the shore. In this process, the tsunami will undergo wave formation and will produce parameters that are also known as tsunami parameters. The parameters present during the tsunami wave transformation process are as follows (Figure 4):

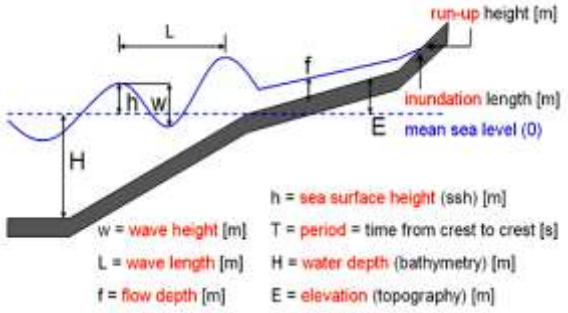

Figure 3: Tsunami parameter (Behren, 2007)

A. Tsunami height

The tsunami height is a vertical distance measured from the sea level to the peak of the wave. The tsunami wave height through deep sea waters is only about ± 2 meters high, but when spreading to the shallow high-pitched tsunami will increase. This process is due to the increasingly shallow beach topography, and the friction of the water body with the base of the beach. The turbulent wave due to the slowdown

will be concentrated followed by the next waves. With accumulated energy able to drive the tsunami as high as tens of meters when it reaches the beach. Coastal-shaped coastal Morphology and estuary are at high risk to receive the maximum tsunami height, this is influenced by the coastline that seems to shape the shape of U and V. Although basically, the coastal areas like the bay and the estuary are calm. The morphology is capable of collecting energy at a maximum point.

B. Run-up

The tsunami run-up is the maximum distance that can be achieved by tsunami waves on land or beach. High rise in water is the vertical distance between the tsunami waves at the beach with the level of sea level. High rise in water and tsunami height depends directly on earthquake magnitude, seafloor morphology, and coastal morphology.

C. Inundation

The inundation is the horizontal distance between the maximum tsunami waves that reach the beach with the coastline. This spillover is influenced by the beach morphology. For the sloping beach, the tsunami spill can reach hundreds of meters away from the shoreline. While for high morphology or hilly beaches, the maximum overflow is only around tens of meters from the shoreline.

D. Travel time

The duration of the tsunami wave is the time required by the tsunami to propagate from the source of a particular point either at sea or at the beach.

The tsunami is also a shallow wave of water where the ratio between water depth and wavelength is very small. This wave propagates with speed that is directly proportional to the depth of the waters. This statement is further clarified by the following relationship:

$$C = \sqrt{gd} \qquad (2)$$

where:

C = shallow water velocity (m / dt)

g = the value of gravity (m / dt2)

= 9.8 m / s2

d = Water depth (m).

The energy transferred to the body of the water dropped at very little value as tsunami waves propagating in deep sea waters moved at very high velocities. For example, if the depth of the sea is 6100 m then the velocity of the wave propagates is 890 km per hour, and this velocity equals the velocity of a fighter jet.

According to Latief (2000), the tsunami velocity is affected by the depth of water. The velocity can reach 800 km/h for deep sea water, 200 km/h for medium deep waters, and 25 km/h for shallow waters and to the shore. When entering the shallow waters and approaching the coast, the tsunami velocity will decrease and experience a slowdown (Figure 5). This slowing process occurs due to reduced depth of water, friction on the sea floor, plant, and building

structures such as houses, walls and so on.

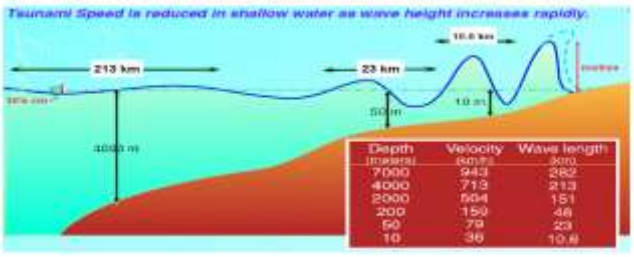

Figure 4: Speed of tsunami propagation to water depth. (*Source: www.ecmwf.org*)

The turbulent wave due to the slowing process will come together with the next waves. This results in a wave height of only ± 1 m in deep sea water to increase to ± 30 m in shallow and coastal waters. The largest wave does not necessarily apply to the first wave, but generally occurs in the first 10 waves.

IV. MATERIALS AND METHODS

The tsunami propagation model used in this study is TUNAMI-N2. This model is basically developed by the Disaster Control Research Center (Tohoku University, Japan) through the Tsunami Inundation Modeling Exchange (TIME) program (Goto *et al.,* 1997). TUNAMI-N2 has been intensively applied in Japan in the study of propagation and tsunami implications against coastal areas in different scenarios (Goto and Ogawa, 1992; Imamura and Shuto, 1989; Shuto and Goto 1988; Shuto *et al.,* 1990). This modelling has also been implemented extensively to simulate propagation and inundation in the Pacific Ocean, the Atlantic Ocean and the Indian Ocean (Yalciner *et al.,* 2000, 2001, 2002; Yalciner, 2004; Zahibo *et al.,* 2003; Tinti *et al.,* 2006).

The tsunami modeling in the Celebes Ocean is considering the shallow water wave theory (Goto and Ogawa, 1982 in Imamura, 2006) where the tsunami propagation simulation is carried out taking into account the elemental friction element. Air friction is neglected because of its very small value and almost no impact. Changes in sea level due to tidal activity are also negligible as the change is very little compared to the high tsunami occurrence. Changes in data entry and detailed analysis were conducted to obtain a simulation scenario of the Tsunami propagation in the Celebes Sea approaching realistic cases.

A. Shallow water theory

The tsunami generated by seafloor movement due to the earthquake is a long wave. Based on wave theory, the velocity of vertical waves of water particles is relatively small compared to gravity velocities, except for cases of tsunami wave propagation (Kajiura, 1963 and Imamura, 2006). As a continuation, the vertical movement of water particles does not affect the distribution of pressure forces. Therefore, it can be explained that the pressure becomes hydrostatic.

Based on the above approach and if the vertical velocity is negligible, the equations of time and momentum observations can be solved for cases involving two dimensions. For cases of tsunami wave propagation in shallow waters, horizontal eddy tubules can be neglected by comparison with basic friction

except for landfill. The equation below is an equation which is based on the tsunami modelling of this study:

$$\frac{\partial \eta}{\partial t}+\frac{\partial M}{\partial x}+\frac{\partial N}{\partial y}=0$$

$$\frac{\partial M}{\partial t}+\frac{\partial}{\partial x}\left(\frac{M^2}{D}\right)+\frac{\partial}{\partial y}\left(\frac{MN}{D}\right)+gD\frac{\partial \eta}{\partial x}+\frac{\tau_x}{\rho}=A\left(\frac{\partial^2 M}{\partial x^2}+\frac{\partial^2 M}{\partial y^2}\right)$$

$$\frac{\partial N}{\partial t}+\frac{\partial}{\partial x}\left(\frac{MN}{D}\right)+\frac{\partial}{\partial y}\left(\frac{N^2}{D}\right)+gD\frac{\partial \eta}{\partial y}+\frac{\tau_y}{\rho}=A\left(\frac{\partial^2 N}{\partial x^2}+\frac{\partial^2 N}{\partial y^2}\right) \quad (3)$$

where D is the value of the overall depth of the waters given by h + η, τx and τy is the basic friction in the direction of x- and y-, A is the horizontal eddy viscosity where assumed to be constant against space, shear stress on surface waves is ignored. M and N are discharged fluxes in x- and y- directions were given by,

$$M=\int_{-h}^{\eta} u\,dz=u(h+\eta)=uD$$

$$N=\int_{-h}^{\eta} v\,dz=v(h+\eta)=vD \quad (4)$$

Basic friction is generally expressed as the following equation which is also an analogy of the uniform flow.

$$\frac{\tau_x}{\rho}=\frac{1}{2g}\frac{f}{D^2}M\sqrt{M^2+N^2}$$

$$\frac{\tau_y}{\rho}=\frac{1}{2g}\frac{f}{D^2}N\sqrt{M^2+N^2} \quad (5)$$

where f is the coefficient of friction. The f value is selected from Manning's coefficient of the coefficient, n which has been determined through civil engineering. The value n can be seen in Table 1.

Table 1: The value of zero friction coefficient (Linsley & Frazini, 1979 in Imamura, 2006)

Base Material	n	Base Material	n
Neat cement, smooth metal	0.010	*Natural channels in good condition*	0.025
Rubble masonry	0.017	*Natural channels with stones and weeds*	0.035
Smooth earth	0.018	*Very poor natural channels*	0.060

The relationship between friction coefficient f and Manning n Coefficient of Coefficients is as follows:

$$n=\sqrt{\frac{fD^{1/3}}{2g}} \quad (6)$$

As the implication f becomes larger when the small D depth (shallow) when it is almost constant. Basic frames can be expressed as follows:

$$\frac{\tau_x}{\rho}=\frac{fn^2}{D^{7/3}}M\sqrt{M^2+N^2}$$

$$\frac{\tau_y}{\rho}=\frac{fn^2}{D^{7/3}}N\sqrt{M^2+N^2} \quad (7)$$

For the modeling done in this study, the basic friction equation used is in equation (5), that is, the n value is selected based on the base state of Table 1.

The model used in this study only focuses on the movement caused by the generation of underwater earthquakes without taking into account other generating elements such as wind and tidal processes. The surface of the sea is also assumed to be constant throughout this modeling process. Accordingly, it is assumed that when n-1 does not apply movement. This can be expressed through the following equation:

$$\eta_{i,j}^{n-1}, \qquad M_{i+\frac{1}{2},j}^{n-\frac{1}{2}}, \qquad N_{i,j+\frac{1}{2}}^{n-\frac{1}{2}} = 0 \tag{8}$$

Estimation of inundation, the water surface height η, originally is equal to the landmark h.

$$\eta_{i,j}^{n-1} = -h_{i,j} \tag{9}$$

B. Domain design

In the process of designing the domain the most basic thing to do is to determine the work space of the simulation. In this study, there are four simulation spaces consisting of columns A, B, C and D. Each of these workspaces has different spatial grid size which also describes the accuracy of the required data. Space is also different where space A is the main domain while space B, C, and D are a subset of space A (Figure 6). Table 2 describes the overall properties and boundaries of the workspace used in this simulation. This method is also known as a nested model.

Table 1: Scale of survey and modeling data

Domain	X Border		Y Border		Matrix grid (X*Y)	Data Accuracy
	Min	Max	Min	Max		
A	116.005°	124.9825°	-2.0025°	7.9875°	400*445	81s
B	117.3850°	118.6675°	3.6300°	4.8675°	172*166	27s
C	117.5825°	118.3625°	3.9325°	4.5600°	313*256	9s
D	117.7833°	118.1658°	4.1333°	4.2708°	460*166	3s

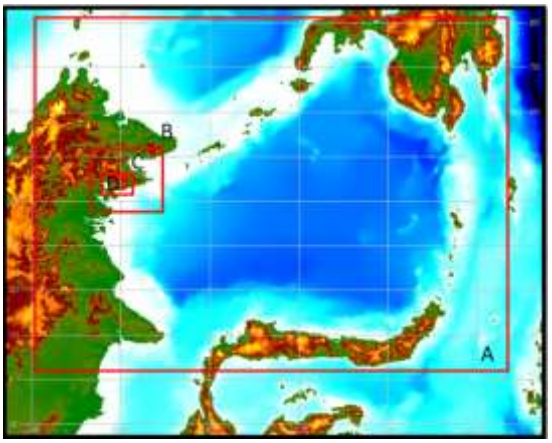

Figure 5: Model space domain consisting of domains A, B, C, D with the accuracy of the data of 3, 9, 27, 81 arcsec respectively

The design determination of this model starts with the smallest grid pause gradually, aiming to obtain optimum grid transfer ratio. In addition, model boundaries are also given attention so as to avoid drastic changes in beach morphology or sea morphology.

To get good simulation results, detailed bathymetric and topographic data are required. At this stage, the study was more selective by combining C-map and NOAA data sources to complement the deep-sea water data used through the ETOPO1 source. Bathymetric data through C-Map sources have high accuracy in coastal areas as these C-Map functions are for navigation and sea traffic. The combination of ETOPO1 resources and refined with C-Map data and NOAA as a whole is in line with the needs and use of TUNAMI-N2. The data used also directly addresses the needs of the study and the area to be modelled.

C. Fault design

After preparing the model domain space, the next process is designing the model design which is also the basic data model. In the design process, the study identifies North Sulawesi Trench as a fault that are at risk of generating tsunamigenic earthquakes and giving a high impact of tsunami damage in the Tawau District especially Tawau City, and North Sulawesi. Based on USGS / NEIC and JMG Malaysia records from 1973 to 2009, there are some records of a series of earthquake events of 7Mw and above occurred in North Sulawesi and Cotabato active faults. In the analysis of the sensitivity of the fault parameters, the best possible study would be to provide the true state of the scenario. Meanwhile, this study still considers the need for hypothetical parameters to analyze any change in parameter values. Therefore, in order to ensure the selection of earthquake resources has a strong justification then the magnitude of the fault jealousy is invoked so that the earthquake identity is unchanged in line with the actual fault identity.

Determination of this hypothetical fault parameter only involves six of the seven parameters and each parameter change is performed systematically with the appropriate interval value. Table 3 describes the parameters and values of the changes involved. Determination of parameter pauses is a rather difficult process as there is no specific value used in the determination. Therefore, the study uses random methods by establishing several possible scenarios with the limitations of the earthquake moment.

Table 3: The value of fault parameters

Slip Magnitud (°)	Length (KM)	Width (KM)	Strike (°)	Dip Angle (°)	Rake Angle (°)	Depth (KM)
15	150	15	240	60	80	30
20	155	20	240	65	85	35
25	160	25	240	70	90	40
30	165	30	240	75	95	45
35	170	35	240	80	100	50

Considering the earthquake distribution around the Celebes Sea, the relevant earthquake location was chosen as the source of the tsunamigenic earthquake for this study which is North Sulawesi. The distance of the earthquakes of North Sulawesi from the Tawau City coast is 520k. Fault location also represents the tsunami scenario for the cause at long distance (Figure 7).

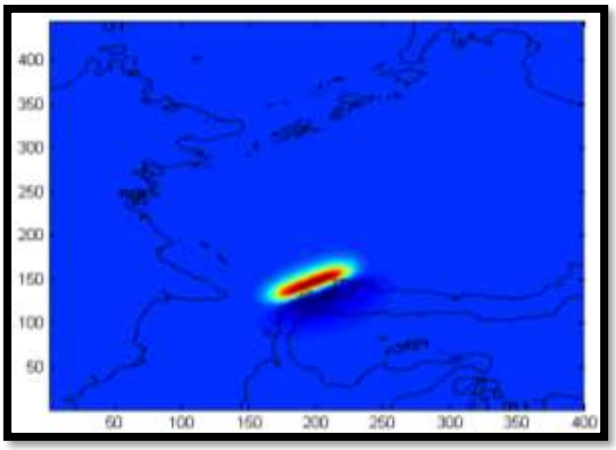

Figure 6: North Sulawesi fault model at risk of tsunamigenic earthquake

D. Observation Station

The findings of modeling data are by hypothetically observing stations taking into account the suitability of the location. Through this study, there are five observation stations (Figure 8) where during this simulation the observation station will record every required

data without changing its position. This aimed to obtain more accurate simulation results without being affected by the change of station location. In this situation, it is to be noted that Tawau City is located on the coast with multiple facilities within four kilometers of the coastline. However, the station location priority is to areas with rapid development and high population density. The determination of this location is generally to illustrate the impact of the entire study area in Tawau City.

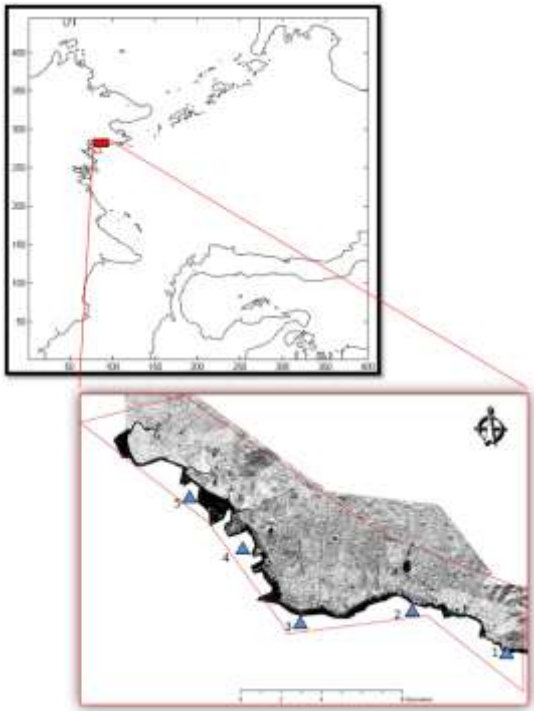

Figure 7: Location of the observation station along Tawau coastline

V. RESULTS AND DISCUSSIONS

The simulation analysis process involves 350 modeling data which consists of six fault parameters, five data scenarios with systematic changes, and each change is observed at five different observation stations. This process is done for faults of North Sulawesi. For the determination of the sensitivity of the fault parameters, the wave height changes for each observation station are recorded and plotted in the graph to obtain the trend of change for each parameter against the height of the tsunami wave.

An analysis of this plotted graph is very important in determining the relationship between tsunamigenic earthquake parameters and the resulting tsunami wave height. Before the sensitivity of the earthquake parameter change was determined, the results of this modeling simulation were first tested whether it had a significant effect on the height of the waves. This process applies simple regression analysis by considering tsunamigenic earthquake parameters as independent variables and wave height as a controlled variable.

An analysis of North Sulawesi Fault case is based on earthquake source in North Sulawesi with 4 hours of simulation time. By recording the maximum height of the wave in each case, the graph of the parameter value against the height of the tsunami wave is plotted for each observation station.

A. Slip Magnitude

Each 5m data change for the magnitude of the slippage and height is plotted. A linear regression model representing the distribution of data x (magnitude of slippage) against y (wave height) is plotted to obtain the association between x and y. Data R2 is obtained for each graph for each plotted station. Figure 9 shows

that the linear regression model for each plotted station is acceptable with a consistent R2 value approaching value one.

The linear regression model's gradient for Observation Station 1 is 0.064. The data at Observation Station 1 shows that each 1m increase in the magnitude of the sliding magnitude will contribute to a high rise of 0.064m waves. For Observation Station 2, the gradient value is 0.061 and shows that the 1m magnitude of the slippage contributes to the increase of wave height of 0.061m. The Observation Station 3 records where each 1m magnitude sliding change will contribute to a wave increase of as high as 0.071m. Whereas the 1m magnitude fluctuations in Observation Station 4 recorded an increase of 0.069m of waves. Observation Station 5 also recorded a waveform of 0.047m per 1m magnitude of slippage.

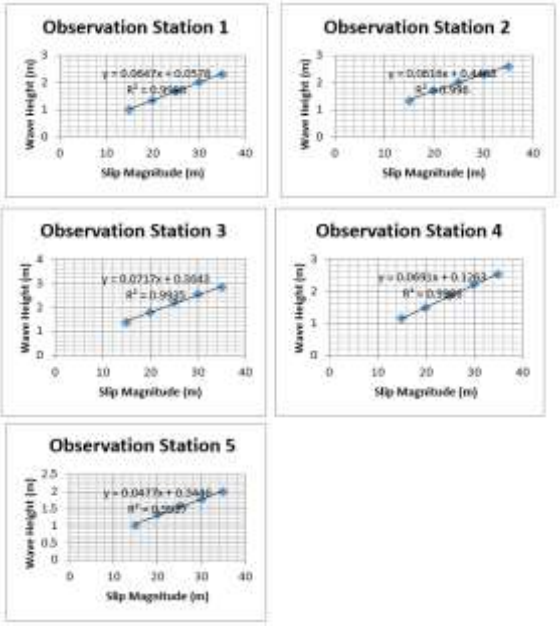

Figure 8: Wave height to slip magnitude graph

B. Fault Length

Each 5km data change for fault length and height is plotted. A linear regression model that represents the distribution of data x (fault length) against y (wave height) is plotted to obtain a connection between x and y. Data R2 is obtained for each graph for each plotted station. Figure 10 shows that the linear regression model for each station that has been plotted is acceptable with a consistent R2 value approaching value 1.

The likelihood of the linear regression model for the fault length parameter for Observation Station 1 shows the value of 0.006. This value explains the influence of longitudinal fault changes on tsunami waves. Each 1km increase in the length of the fault will contribute to a high rise of waves as high as 0.006m. For Observation Station 2 the waveform changes to the recorded fault length changes are the same as Observation Station 1 which is a slope of 0.006. Observation Station 3 records every 1km long fault change will contribute to a high-altitude alteration of 0.005m. Observation Station 4 recorded an increase of 0.003m high waves per 1km of fault length change. For Observation Station 5, every 1km of the length of faulting will cause a high increase of oozes of 0.005m.

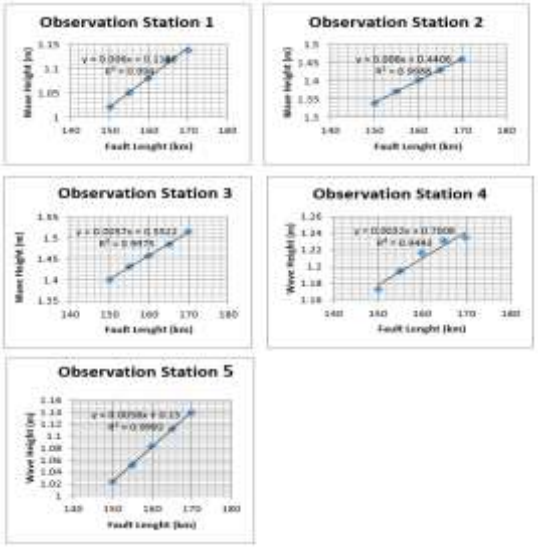

Figure 9: Wave height to fault length graph

C. Fault Width

Each 5km data change for fault width and height is plotted. A linear regression model representing the data of x coating (fault width) against y (wave height) is plotted to obtain the relationship between x and y. Data R2 is obtained for each graph for each station that has been plotted. Figure 11 shows that the linear regression model for each plotted station is acceptable with the R2 value which is consistently approaching the value of 1.

The linear regression fatigue model for this fault width parameter explains the effect of the change in the width of the fault to the change of tsunami wave height. Observation Station 1 shows the value of 0.049 for the linear regression model of the gradient and this can be defined as each increase of 1 km of fault width will contribute to the increase of high waves up to 0.049m. Observation Station 2 records each 1km increase in the width of the fault will increase the rise of high waves of 0.051 m. The Observation Station 3 records every 1km of the transformed fault width will give rise to 0.06m high waves. For Observation Station 4 1km width will affect waveform of 0.058m and Observation Station 5 of 0.04m wave height.

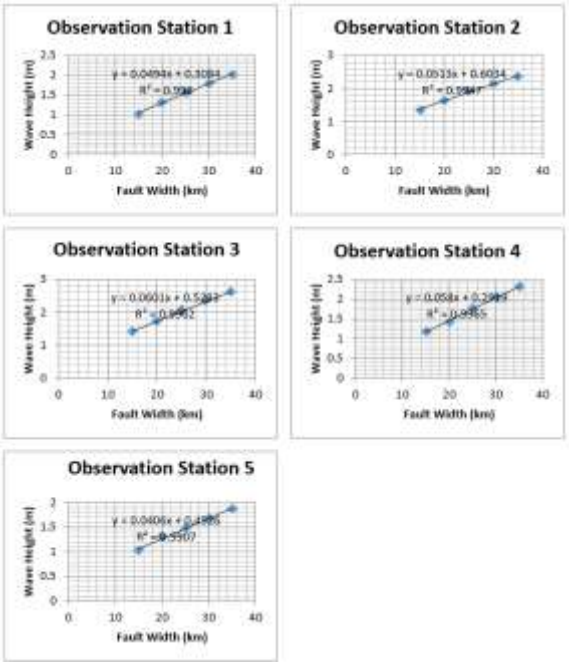

Figure 10: Wave height to fault width graph

D. Dip Angle

Each 5 ° change of data for the junction and height angle is plotted. A linear regression model representing the x-data distribution (juncture angle) against y (wave height) is plotted to obtain an association between x and y. Data R2 is obtained for each graph for each plotted station. Figure 12 shows that the linear regression model for each station that has been plotted is acceptable with R2 value approaching value 1.

The linear regression model's gradient for this juncture parameter describes the effect of junctions on the change of tsunami wave height. Based on Figure 12, early research found that the

correlation between the junctions and the height of the wave is inversely proportional. Observation Station 1 records the value of the gradient is -0.006, this clarifies that each increase of 1 ° junction angle will contribute to a decrease in the height of the waves by 0.006m. For Observation Station 2 the gradient value shows that every 1 ° angle increase will cause a wave drop of 0.014. The Observation Station 3 recorded a wave drop of 0.019m for every 1 ° angle change. Observation Station 4 shows that the height of the wave will decrease 0.017m each increase of 1 ° junction angle. Observation Station 5 shows a change in wave height drops of 0.008m for each 1 ° increment angle.

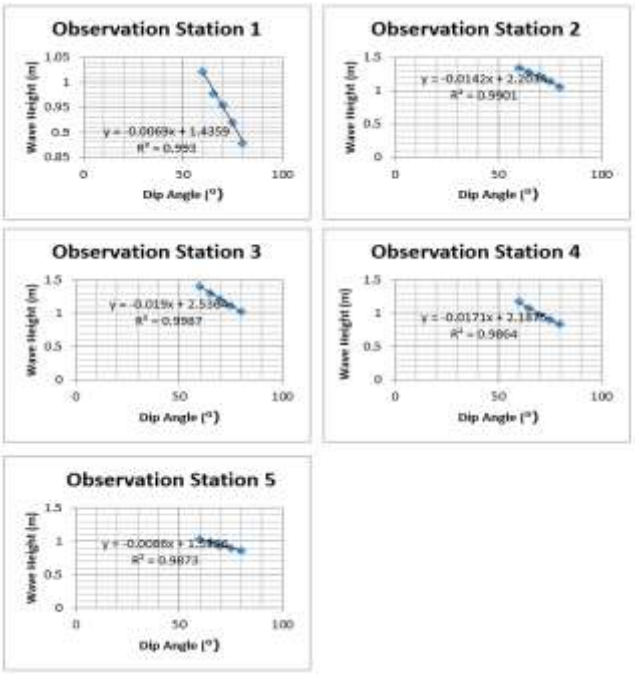

Figure 11: Wave height to dip angle graph

E. Rake Angle

Each 5 ° data change for the point of view and height is plotted. A linear regression model representing the x-distribution of data (auxiliary angle) against y (wave height) is plotted to obtain an association between x and y. Data R2 is obtained for each graph for each plotted station. Figure 13 shows that the distribution of data is random and does not show any relationship trends between the angle of movement and the height of the wave.

This analysis is explained by the linear regression model that has been made, where the R2 value of Observation Station 1 is 0.005, Observation Station 2 is 0, Observation Station 3 is 0.013, Observation Station 4 is 0.372 and Observation Station 5 is 0.072. The R2 value recorded by the change in the angle of the switch is away from the value of 1 and there is no connection between the height of the wave and the change in the angle of the switching angle. This means that any 1 ° increase in the point of view will give the value of the wave height that fluctuates and does not either increase or decrease.

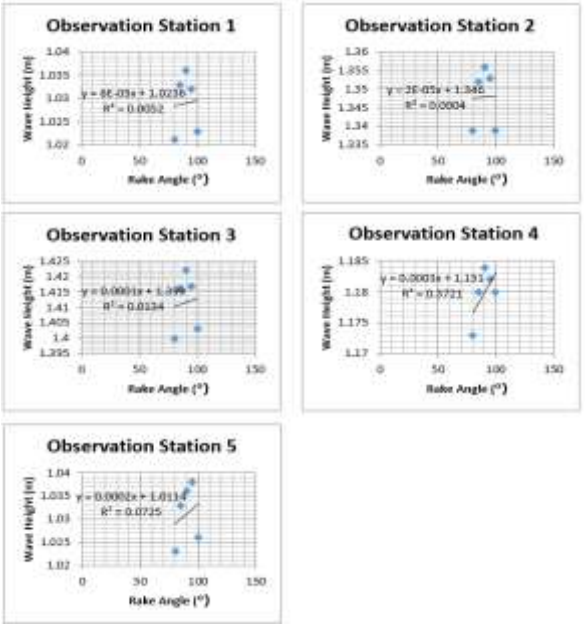

Figure 12: Wave height to rake angle graph

F. Depth

Each 5km data change for fault depth and height is plotted. A linear regression model that represents the distribution of data x (fault depth) against y (wave height) is plotted to obtain a connection between x and y. Data R2 is obtained for each graph for each plotted station. Figure 14 shows that the data distribution for each station is consistent. However, the gradient value change which explains the relationship between the fault and the wave height changes to large errors. It is generally worth noting that the relationship between the depth of the fault and the height of the wave is inversely proportional.

Each 1km depth of fault will contribute to wave drops of 0.011m, 0.015m, 0.016m, and 0.016 respectively for Observation Station 1, Observation Station 2, Observation Station 3 and Observation Station 4. If observed these changes are in a consistent range. For observation stations 5, there was an increase of 0.005 for every 1km depth of fault change.

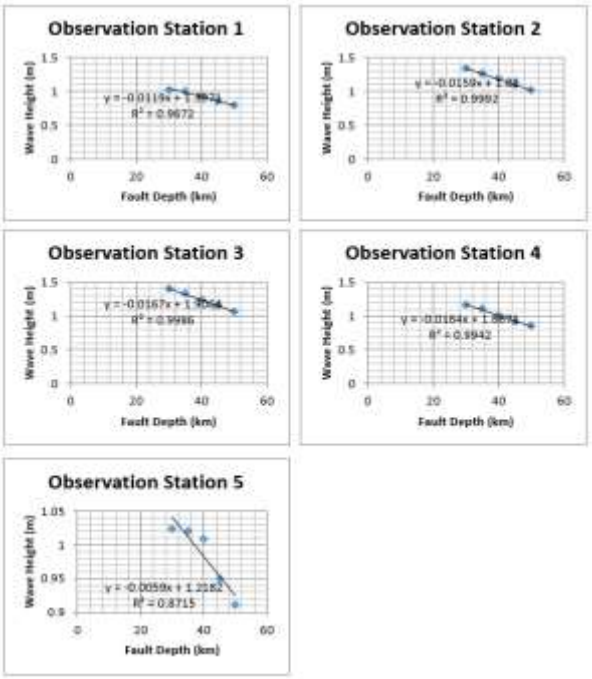

Figure 13: Wave height to fault depth graph

VI. SUMMARY

Through the analysis of modelling simulation results, it can be identified that two of the six parameters tested provide a consistent influence of the change in the magnitude of the slippage and the fault width. The slippage magnitude recorded a wave height change of 0.06m for change of 1m magnitude fluctuations for the case of North Sulawesi Fault. For fault width it affects wave height change of 0.05m each 1km fault change for case North Sulawesi.

For long-fault parameters, the change in the North Sulawesi Fault case is very small at 0.005 per 1km fault length change. The slip magnitude also provides insignificant data on wave height changes where the North Sulawesi Fault case gives rise to angular rise effect is inversely proportional to altitude and this is totally contrary to the data obtained in the Cotabato Siberian case even though the

gradient value obtained is consistent. This scenario also applies to data for fault depth parameters. Finally, it is the parameter of the point of view, at the beginning of the analysis again indicates that the parameter of the point of view does not give any relation to the resulting wave height of the tsunami. This is explained by an easy linear regression analysis where the regression model plotted through the results of the data collection is not acceptable to the R2 value that is away from the value of one.

[1] Goto, C. & Ogawa, Y. (1992). Numerical method of tsunami simulation with the leap-frog scheme (Translated for the Time Project by Shuto, N., Disaster Control Research Center, Faculty of Engineering, Tohoku University in June 1992).

[2] Goto, C., Ogawa, Y., Shunto, N., Imamura, F. (1997). Numerical method of tsunami simulation with leap-frog scheme. (IUGG/IOC Time Project), IOC Manual, UNESCO, No. 35.

[3] Hutchinson, S.C. (1989). Geological evolution of South East Asia. Oxford Monographs on Geology and Geophysics, 13, 23-29.

[4] Hall, R. (2002). Cenozoic geological and plate tectonic evolution of SE Asia and the SW Pacific: Computer based reconstructions, model and animation. J.Asian Earth Sciences, 20(4), 353-431.

[5] Imamura, F. & Shuto, N., Numerical simulation of teh 1960 Chilean tsunami. In: Proceeding of japan-China (Taipei) Joint seminar on Natural Hazard Mitigation, Kyoto, Japan.

[6] Johnston, A. (1996). Seismic moment assesment of the earthquake in stable continental regions – III New Madrid 1811-1812, Charleston 1886 and Lisbon 1755. Geophysical Journal International 126, 314-344.

[7] Lin, J. & Stein, R.S. (2004). Stress triggering in thurst and subduction earthquake, and stress intersection between the southern San Andreasand nearby thrust and strike-slip faults. Journal of Geophysical Research. 109, 1-19.

[8] Liu, P.L.-F., Woo, S.-B., Cho, Y.-S. (1998). Computer Program for Tsunami Propagation and Inundation, sponsored by National Science foundation <http://ceeserver.cee.cornell.edu/pll-group/comcot_down.htm>

[9] Lockridge, P. A., Lowell, S., Whiteside, L. A. & Lander, J. F. (2002). Tsunami and tsunami-like waves of the Eastern United States. International Journal of Tsunami Hazards. 20(3), 120-157.

[10] Mei, C. C. (1989). The Applied Dynamic of Ocean Surface Waves. World Scientific, Singapore, p. 740.

[11] Manisha, L. & Smylie, D. E. (1971). The displacement fields of inclined faults. Bulletin of the Seismological Society of America, 61(5), 1433-1440.

[12] Moreira, V. S. (1985). Seismotectonics of Portugal and its adjacent area in the Atlantic. Tectonophysics, 117, 85-96

[13] Mitchel1, G. W., Becker, M., Angermann, D., Reigber, C. & Reinhart, E. (2000). Crustal motion in E- and SE-Asia from GPS measurements. Earth Planets Space, 52(10), 713-720.

[14] Natawidjaja, D. H. & Triyoso, W. (2007). The Sumatera Fault Zone: From source to Hazard. In: Proceedings of 2007 Workshop on Earthquake and Tsunamis: Fromsource to Hazard, National University of Singapore, 7-9 March 2007.

[15] National Earthquake Information Center, 2007. Earthquake <databas.http:/neic.usgc.gov/neic/epic.>

[16] NGDC (National Geophysucal data Center), 2007. World-wide tsunamis, 2000 BC to 2010. NOAA. <http://www.ngdc.noaa.gov/seg/hazard/tsuintro.html>

[17] Raj, J. K. (2007). Tsunami threat to coastal areas of Sabah, East Malaysia. Geological Society of Malaysia, 53, 51-57.

[18] Jamaluddin, Tajul Anuar., Komoo, Ibrahim., Leman, Mohd Shafeea., Tongkul, Felix., Latief, Hamzah., Sian, Lim Choun. &

R. Gusman, Aditya. (2007). Policy And Planning Respone for Earthquake and Tsunami Hazards In Malaysia – Preliminary results.

[19] Tongkul, F. (1992). The ranau Earthquake:possible causes. Sabah Society Journal, 9(4), 315-322.

[20] Ward, S.N. (2002). Tsunamis. Encyclopedia of Physical Science and Technology-Academic Press, 17, 175-191.